We are IntechOpen,
the world's leading publisher of
Open Access books
Built by scientists, for scientists

4,800
Open access books available

122,000
International authors and editors

135M
Downloads

154
Countries delivered to

Our authors are among the

TOP 1%
most cited scientists

12.2%
Contributors from top 500 universities

BOOK CITATION INDEX

CLARIVATE ANALYTICS

INDEXED

WEB OF SCIENCE™

Selection of our books indexed in the Book Citation Index
in Web of Science™ Core Collection (BKCI)

Interested in publishing with us?
Contact book.department@intechopen.com

Numbers displayed above are based on latest data collected.
For more information visit www.intechopen.com

Sintering to Transparency of Polycrystalline Ceramic Materials

Marta Suárez[1,2], Adolfo Fernández[1,2],
Ramón Torrecillas[2] and José L. Menéndez[2]
[1]ITMA Materials Research
[2]Centro de Investigación en Nanomateriales y Nanotecnología (CINN).
Consejo Superior de Investigaciones Científicas (CSIC) –
Universidad de Oviedo (UO) – Principado de Asturias
Spain

1. Introduction

There is currently a high demand for advanced materials for different types of applications (see Fig. 1.1) in which besides a high mechanical performance, a partial or total transparency in a given spectral range is required. Transparent ceramics become more and more important for applications in which materials are subject to extremely high mechanical and thermal stress in combination with optical properties. More recently, interest has focused on the development of transparent armor materials (ceramic) for both military and civil applications. Also, the development of new optoelectronic devices has extended the use of ordinary optical materials to new applications and environments such as temperature (IR) sensor, optical fiber communications, laser interferometers, etc. A considerable fraction of these new devices operates in aggressive environments, such as ovens, radiation chambers and aerospace sensors. In such cases, the sensitive electronic component must be preserved from the extreme external condition by a transparent window. Transparent and coloured ceramics are also often used as wear and scratch resistant parts such as bearings and watch glasses as well as for their aesthetic Properties in synthetic opals and rubies.

In science and technology the word transparent is used for those components that show clear images regardless of the distance between the object and the transparent window. Clear transparency is achieved when after transmission through the window the light does not undergo noticeable absorption or scattering. This applies, for example, to some glasses, single-crystalline and polycrystalline transparent ceramics.

Most of ordinary optical transparent materials, glasses, polymers or alkali hydrides are soft, weak and/or brittle. Figure 1.2 shows the transmittance spectrum of BK7, a commercial glass widely used for visible optics. However, this material presents a strong absorption in the IR range making it of no use for this spectral range. Furthermore, this material shows a very low melting point (559ºC) so it cannot be used at high temperature.
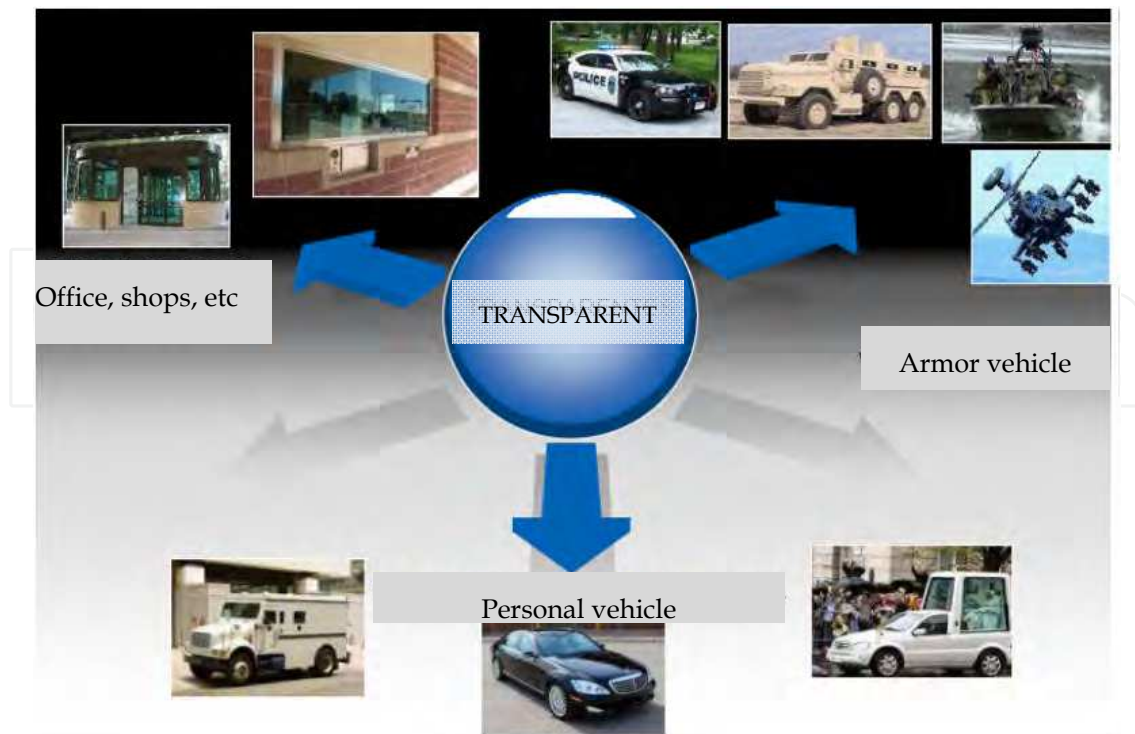
Fig. 1.1. Applications in which transparent materials are required.

However, some ceramic materials, such as corundum, spinel, yttria and YAG, do not show any absorption in a large range between IR and UV (see Fig. 1.2) and are suitable to work under extreme conditions due to their chemical stability and high mechanical performance. Many transparent ceramics are single crystal materials grown from the melt or by flame processes. However, the growth and machining of single crystals is an expensive task, which largely limits their scale up of production and, therefore, their range of applications.
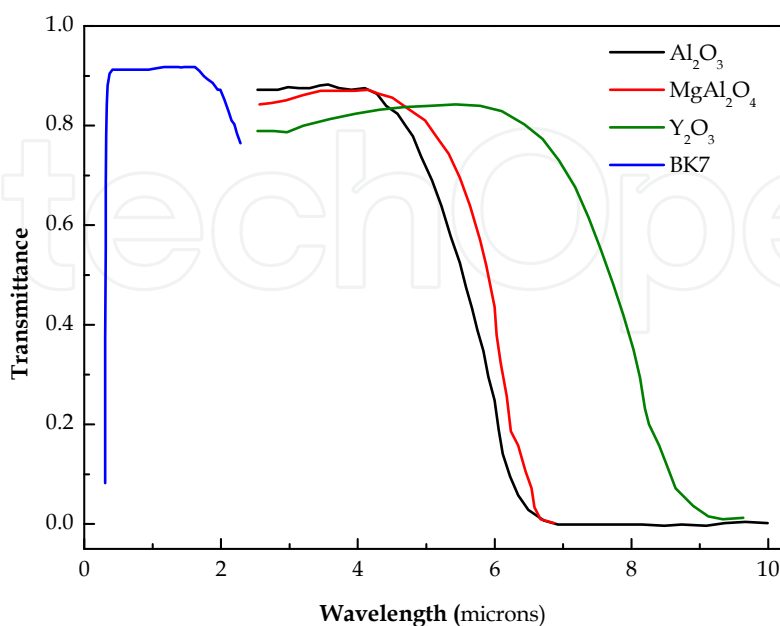

Fig. 1.2. Transmittance spectra of different materials.

Most of these problems can be solved with the use of polycrystalline materials as they show similar mechanical, chemical and thermal stability compared to single crystals and can be produced in complex shapes and are not size limited as single crystals. Among them, only a small number of materials such as MgF_2, ZnS and ZnSe are used for optical applications, but generally their use is limited to coatings and thin films and their mechanical behavior is not appropriate. For this reason, the current trend moves towards the production of polycrystalline transparent ceramics which, by providing more versatility to properties and to the production of complex shapes, will broaden the fields of application. Compared to single crystals, polycrystalline materials have a complex microstructure consisting on grains, grain boundaries, secondary phases and pores. These factors have a great influence on the optical properties, resulting in transparent, translucent or opaque materials, as can be seen in figure 1.3.
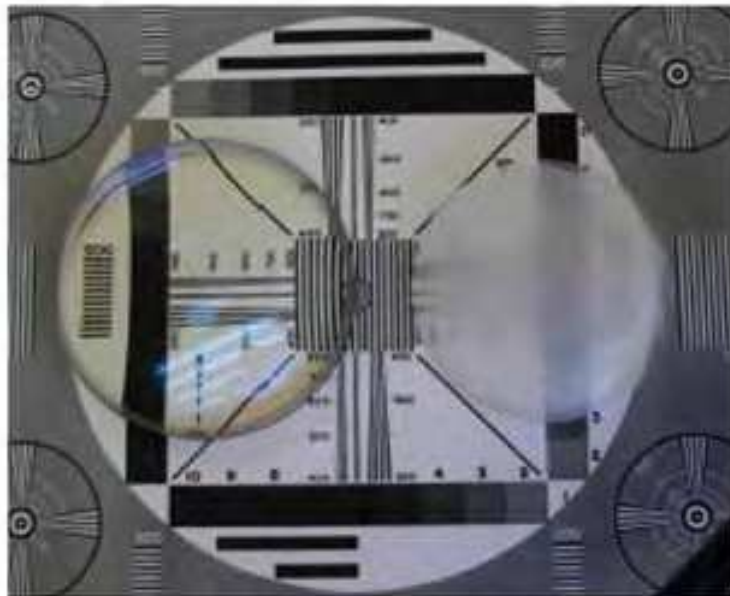

Fig. 1.3. Light scattering on polycrystalline ceramics.

In order to become transparent, the ceramic should be poreless and have optically perfect crystal boundaries and crystals. The surface of a pore is a boundary between phases with sharply different optical properties, and therefore, it intensely reflects and refracts light. A large number of pores makes ceramics opaque. Pores may be intercrystalline or intracrystalline. The elimination of intracrystalline pores, even if they are submicron in size, is a much longer process than elimination of closed intercrystalline pores. Intercrystalline pores occur at crystal boundaries which are sinks of vacancies, and this makes their removal easier. The presence of a second phase on the crystal boundaries which has different optical properties from the main crystalline phase leads to reflection and refraction of light and makes the ceramic less transparent. For this reason, transparent ceramics are obtained from raw material of high purity and the amount of additive is chosen so that they completely dissolve in the solid solution with the main phase.

The crystals in ceramics should be optically perfect, this is the absence of optical defects: pores, inclusions of the second solid phases, aggregate boundaries, and dislocations. In

ceramics from optically anisotropic crystals an additional scattering of light arises on the boundaries because of their arbitrary crystallographic orientation.

The amount of light scattering therefore depends on the wavelength of the incident radiation, or light. For example, since visible light has a wavelength scale on the order of hundreds of nanometers, scattering centers will have dimensions on a similar spatial scale. Most ceramic materials, such as alumina and its compounds, are formed from fine powders, yielding a fine grained polycrystalline microstructure which is filled with scattering centers comparable to the wavelength of visible light. Thus, they are generally opaque as opposed to transparent materials. The degree of transparency also depends on the thickness of the component. These losses increase with growing thickness and result in translucent behavior. Transparency, which is independent of the thickness, is only possible for materials with an in-line transmission close to the theoretical maximum. These materials do not cause losses by absorption or scattering. These considerations lead us to the requirements to be observed by manufacturers of transparent ceramics.

2. Ceramic materials

Different materials have been proposed to prepare transparent ceramics such as alumina, spinel, yttria, AlON, YAG, etc (see Fig. 2.1).
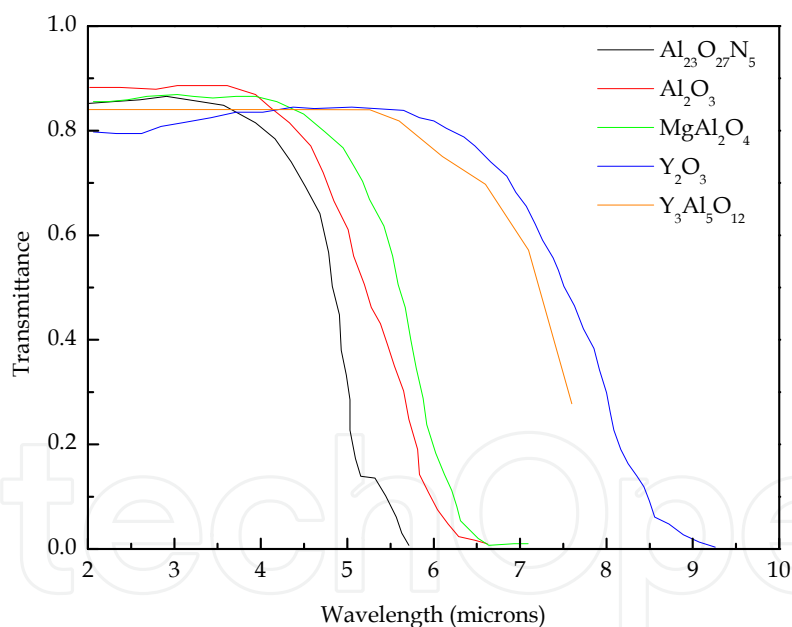

Fig. 2.1. Transmittance spectra of ceramic materials.

Aluminium oxynitride spinel ($Al_{23}O_{27}N_5$, AlON) is a cubic material and one of the leading candidates for transparent armor. This material is very useful for aircraft, missiles, IR and laser windows, etc (Mccauley et al., 2009) as it is stable up to 1200°C, relatively light weight and resistance to damage due to oxidation or radiation. AlON is optically transparent (≥80%) in the near ultraviolet, visible and near infrared regions of the electromagnetic spectrum (see Fig. 2.1). It is four times harder than fused silica glass, 85% as hard as sapphire and nearly 15% harder than magnesium aluminate spinel (table 1). The

incorporation of nitrogen into aluminium oxide stabilizes a crystalline spinel phase, which due to its cubic crystal structure and unit cell, is an isotropic material which can be produced as a transparent ceramic nanomaterial. T. M. Hartnett et al (Hartnett et al., 1998) have obtained transparent AlON in the IR region by sintering at 1880°C in a graphite oven. However, this material is not stable under low N_2 pressure and at temperatures higher than 1640°C. Furthermore, this material is susceptible to oxide in air atmosphere at temperatures higher than 1200°C making it not useful as projection lamps (Wei, 2009).

Material	Strength (MPa)	Knoop hardness (Kg/mm2)	Modulus (GPa)	Density (g/ml)	Melting point (K)
AlON	300	1950	323	3.68	2425
Sapphire	700	1500-2200	345-386	3.98	2300
Yttria	150	720	174	5.03	2430
Spinel	100-200	1400	273	3.58	2400
YAG	200-250	1215	300	4.55	1950
ZrO_2	210	1100	180-200	6.52	2128

Table 1. Physical properties of ceramic materials.

Zircona (ZrO_2) is a material with a cubic structure that can be used as a transparent material in different fields: domestic, industrial and military. It is not amongst the hard ceramics (table 1), and its high refractive index near 2.2 is similar to some perowskites. This may explain why few investigations have been published on sintered (polycrystalline) transparent ZrO_2. Single crystals of cubic zirconia are, however, important as artificial gemstones. Their high refractive index gives rise to a high degree of brilliance that comes close to diamonds. In the future the flexibility of powder technology in producing more complex shapes may stimulate the substitution of zirconia single crystals by sintered transparent decorative and optical products. Peuchert et al., (2009) have obtained a transparent material with 65% transmittance at 600 nm using vacuum atmosphere followed by hot isostatic pressing using titanium oxide as sintering aid.

Yttrium oxide (Y_2O_3) is another material with a cubic structure that can be used on pipes for discharge lamps or heat-resistant windows due to its corrosion resistance, thermal stability and transparency in a wide range of the electromagnetic spectrum (figure 2.1). Similarly, when introducing rare earths in its structure, it can be used as the active medium in solid-state lasers. Lukin et al., (1980) have obtained transparent yttria after sintering at 1900°C under vacuum. Anderson (1998) has developed a ceramic $Nd:Y_2O_3$ by conventional sintering. Greskovish et al., (1973) have developed a laser $Y_2O_3:Nd^{3+}$ doped with ThO_2. La_2O_3 doped Y_2O_3 is of interest for IR applications because it is one of the longest wavelength transmitting oxides. It is a refractory with a melting point of 2430°C and has a moderate thermal expansion coefficient (table 1). A major consideration is the low emissivity of yttria, which limits background radiation upon heating. In particular, lasers with ytterbium as dopant allow the efficient operation both in CW (Kong et al., 2005) and in pulsed regimes (Tokurakawa et al., 2007).

Magnesium aluminate spinel ($MgAl_2O_4$) is a transparent ceramic with a cubic crystal structure. This material shows an excellent optical transmission from 0.2 to 5.5 micrometers and high values of hardness (table 1) making it useful for a wide range of optical applications, including electronic and structural windows in the IR region (see Fig. 2.1). Optical quality transparent spinel has been produced by sinter/HIP, hot pressing, and hot press/HIP operations, and it has been shown that the use of a hot isostatic press can improve its optical and physical properties (Patel et al., 2000). Several authors have worked on obtaining materials of transparent spinel, as the case of Cook et al., (2005). These authors have synthesized spinel powders which subsequently formed by cold isostatic pressing and sintered in a hot pressing machine by applying a mechanical pressure of 4 MPa obtaining a transparent material. Lu et al., (2006) have obtained a transparent spinel material after sintering at low temperature and high pressure (2-5 GPa). Morita et al., (2008) have obtained a transparent spinel material after sintering at 1300ºC in plasma sintering equipment (Spark Plasma Sintering, SPS), reaching 47% of transmittance at 550nm. Spinel offers some processing advantages over AlON such as the fact that spinel is capable of being processed at much lower temperatures than AlON, and has been shown to possess superior optical properties within the infrared (IR) region.

Yttrium aluminium garnet ($Y_3Al_5O_{12}$, YAG) is a polycrystalline material with has a cubic structure that can be used in structural (table 1) and functional applications. YAG has been considered a prime candidate for its use as a matrix in oxide-oxide composites in gas turbine engines (Mah et al., 2004). Also, it can be used as substrate for dielectric components, prisms and mirrors, as a part of discharge lamps, high intensity lamps as well as an active medium for the production of lasers (Ikesue et al., 1995), since it is able to accept trivalent cations in its structure, especially rare earths and transition metals. In this sense, YAG can be doped with Yb^{3+} for diode-laser (Takaichi et al., 2003), with Er^{3+} (Qin et al., 2004) widely used in medical applications or Eu^{3+} (Shikao et al., 2001) used as cathode ray tube. Finally, Nd^{3+} doped YAG is one of the most popular laser materials (Savastru et al., 2004). Due to its high thermal conductivity has been widely used in commercial, medical (ophthalmology, cosmetic, dental, etc), military and industry since its discovery in 1964. Three stable phases exist in the Y_2O_3–Al_2O_3 system: an orthorhombic perowskite$YAlO_3$ ("YAP") with an Y/Al ratio 1:1, an alumina-rich cubic garnet $Y_3Al_5O_{12}$ ("YAG"), and an yttria rich monoclinic phase with composition $Y_4Al_2O_9$ ("YAM"). Wen et al., (2004) have obtained a transparent polycrystalline material with a transmittance of 63% in the visible range and 70% in the IR region, using a solid state reaction of alumina and yttria and after sintering at 1750ºC in vacuum atmosphere (see Fig. 2.1 for transparency in the IR). Reverse-strike coprecipitation is a common synthesis route for multicationic systems (Li et al., 2000a). Li et al., (2000b) have synthesized a material by the reverse coprecipitation route using aluminum and yttrium nitrates as precursors. The material was sintered at 1700ºC in vacuum.

Traditionally, alpha alumina (α-Al_2O_3) has been considered one of the most widely used structural ceramics as basic matrix in many industrial applications, due to its good mechanical properties (table 1), refractory character and its chemical stability in harsh environments. Also, α-Al_2O_3 presents no absorption (see Fig. 2.1) from the near UV (>0.2 μm) until the IR range (> 5 μm). However, due to the birefringent character of alumina, an additional light scattering directly related to the grain size takes place in polycrystalline materials. This light scattering is originated at the boundaries between two alumina grains

with different crystalline orientations. Two approaches can be followed to minimize/reduce this scattering: (1) increasing the texture of the polycrystalline material during the forming stage to minimize the misorientations between grains (2) decreasing the grain size as much as possible, which usually implies starting with nanometer sized alumina particles and often making use of non conventional sintering techniques, such as microwave (Jiping Cheng et al., 2002) or spark plasma sintering. However, since Coble´s work in the 60´s (Coble, 1962), the possibility of using other ceramic materials than the cubic ones for optical applications was demonstrated.

One way to avoid grain growth during sintering and obtain denser materials with reduced porosity is based on the modification of the diffusion mechanisms at high temperature by the introduction of second phases in grain boundaries or by doping with various elements that change the state of the charges at the grain boundary. In the case of alumina many additives have been proposed, mainly metal oxides (NiO, CoO, ZnO, SnO_2, Y_2O_3, MgO, ...) (Budworth, 1970). Magnesia (MgO) (Shuzhi et al., 1999) is one of the most used doping agents in the case of alumina as it inhibits the grain growth and promotes the development of a more uniform grain structure. The role of MgO has been widely studied since the work of Coble in the 60's, indicating that small additions of MgO ($\leq$ 0.25%) allowed obtaining alumina with a density close to theoretical. Bennison and Harmer (1990a) have also studied the role of MgO in the sintering of alumina, highlighting the effect it has on all the parameters that control the sintering of alumina. Handwerker et al. (1989) have also proposed that the addition of magnesia to alumina reduces the chemical heterogeneity due to the presence of impurities, reducing or eliminating the liquid phase generated by the abnormal growth of grains. Jiping Cheng et al., (2002) studied the influence of the presence of MgO on the transparency of alumina and observed that using MgO as sintering aid allows obtaining alumina samples with a more uniform grain size (equiaxed) and no porosity after microwave sintering.

3. Processing and sintering of transparent ceramic materials

Although many transparent ceramics are single crystal materials, transparent polycrystalline ceramics have different advantages such as low price, ease of manufacture, mass-production and more versatility in properties. Furthermore, the capability of producing complex shapes could broaden the fields of application.

The classical issues of ceramic processing are related with powder quality, purity, defect free processing and elimination of minor defects and pores. When the aim is to reach transparency, requirements will be similar from a qualitative point of view but noticeably more restrictive from a quantitative point of view. In addition, microstructural features such as maximum pore and grain size (the latter for birefringent materials) are critical in scattering process. The requirements for these parameters depend on the wavelength at which transparency is desired. In general, as it will be discussed in section 4, it is assumed that defect size must be < $\lambda/10$ in order to obtain transparent materials.

Then, in this chapter the processing and sintering techniques most widely used in ceramic manufacturing will be revised, describing the key parameters to be controlled and their effect on the optical properties of the final material.

Ceramic fabrication methods can be classified in different categories depending on the starting materials involved (gas, liquid or solid phase). Polycrystalline ceramics are usually manufactured by compacting powder to a body which is then sintered at high temperatures. The geometry, production volume and characteristic requirements for the component govern the choice of manufacturing process. Alternatively, ceramic materials can be simultaneously formed and sintered when pressure assisted sintering techniques are used (see Fig. 3.1).
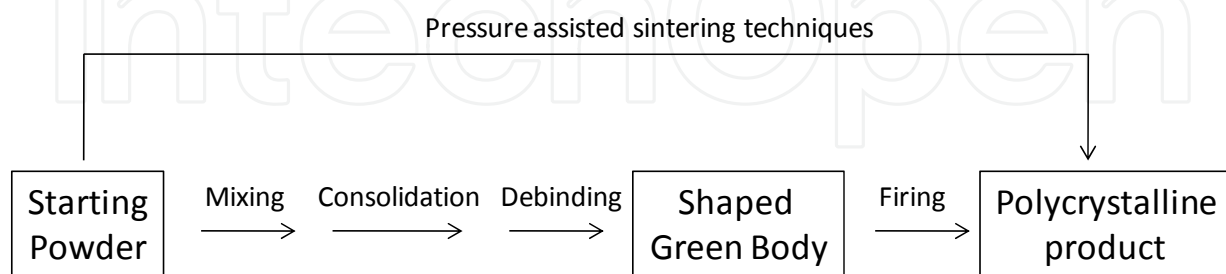
Fig. 3.1. Flow chart for the production of polycrystalline ceramics.

Polycrystalline ceramic processing

The processing steps involved in conventional fabrication of ceramics can be divided in two main parts; formation of green body and firing, and both of them must be carefully controlled in order to avoid residual porosity in the final material.

In the first part, the preparation of shaped green body from ceramic powders, three operations can be identified: mixing, consolidation and debinding. Mixing process includes the preparation of stable slurries from ceramic powders by addition of dispersants or pH controllers and the incorporation of binders and other additives. Consolidation can be done directly from wet slurries or after preparing conditioned powders. Finally, a debinding process for removing the additives used in previous actions before sintering is required.

Although the properties of the starting ceramic powders also play an important role in their behaviour during shaping and sintering, in this review the different ceramic powder synthesis methods will not be described. The description will be focused on the influence of the different processing steps starting from commercial raw materials.

Wet processing of ceramic powders is usually done in order to avoid the formation of undesired powder aggregates that could be responsible of microstructural defects in the final material. As it has been previously mentioned, when the aim is to obtain a transparent material, the critical flaw size above which an important loss of transmittance is observed is very small.

In the processing of ceramics, colloidal suspensions, consisting of a dispersion of solid particles in a liquid, are of particular interest. They are being used increasingly in the consolidation of ceramic powders to produce the green body. Compared to powder consolidation in the dry state, colloidal methods can lead to better packing uniformity in the green body which, in turn, leads to a better microstructural control during firing. Moreover, colloidal suspensions are usually prepared in order to obtain conditioned powders to be consolidated by dye pressing.

Stability of colloidal suspensions depends on particle size and their surface properties. The particles must not be too large otherwise gravity will produce rapid sedimentation. On the other hand, if the attractive force between the particles is large enough, the particles will collide and stick together, leading to rapid sedimentation of particle clusters.

Flocculation will therefore occur unless some process is promoted to produce repulsion between the particles which is sufficiently strong to overcome the attractive force. There are several ways for achieving this, but the most commonly used are:

1. Electrostatic stabilization in which the repulsion between the particles is based on electrostatic charges on the particles
2. Steric stabilization in which the repulsion is produced by uncharged polymer chains adsorbed onto to the particle surfaces
3. Electrosteric stabilization, consisting of a combination of electrostatic and steric repulsion, achieved by the adsorption of charged polymers (polyelectrolytes) onto the particle surfaces.

Rheological measurements are widely used to characterize the properties of colloidal suspensions. They can be used as a method of analysis as, for example, in determining the optimum concentration of dispersant required to stabilize a suspension by measuring the viscosity of the suspension as a function of the concentration of dispersant added.

Once the stable colloidal suspension is prepared, two alternative processes can be distinguished; direct consolidation in order to form a green body or drying under controlled conditions in order to produce a ready to press powder.

In the first case, the processes are known as colloidal forming techniques and their interest is due to the complete deagglomeration of starting powders, reducing the generation of defects. However, other limitations such as difficulties for obtaining larger or complex parts with simultaneously thin and thick cross sections due to density gradients in the green body or problems like the differential sedimentation due to the particle size distribution in the starting powders are found. Slip-casting will be described as an example of colloidal forming technique.

Slip-Casting

Slip casting, with or without pressure, constitutes an ideal combination of dewatering and shaping. As much of the slurry liquid at or near the mould surface is absorbed in the pores in the mould, a layer of solid is formed by the interlocking solid particles in the region near the mould surface. As the process continues, this solid layer increases so long as the mould pores continue to absorb the liquid of the slurry.

The biggest advantage of this process is its versatility in terms of shape, size and materials applicability. It can also accommodate a range of particle sizes, working with typical particle sizes from a fraction of a micron (green densities of ~ 40-50%) to several microns. It can also work fairly well with finer, nanoscale particles. A comparison between slip casting and uniaxial pressing of yttria ceramics show how the minimization of density gradients in green bodies prepared by slip casting allows obtaining more homogeneous materials in terms of translucency and microstructure (J. Mouzon et al., 2008).

However, slip casting has limitations, which, from an operational point of view, are primarily its slow casting rates, with thickness proportional to the square root of casting time, and hence increased cost of casting and of drying to avoid cracking, as well as costs for preparing and maintaining a large mould inventory and facilities for mould storage and drying. Using pressure to accelerate the dewatering process improves the productivity of the process. The main difference in comparison with slip casting is that the water is not removed by capillary suction (negative pressure in the plaster mould) but by pressurisation (positive slip pressure). Control of the filtration process is based on four parameters; the pressure differential on the body, the liquid-medium viscosity, the specific surface area of the slip's solids content and the body porosity (body formation is dependent on the permeability of the layer of body that has already formed from filtered material).

In order to solve those problems a great diversity of advanced forming techniques has been developed. Amongst them, aqueous injection moulding, centrifugal slip casting, direct coagulation casting, electrophoretic casting, gelcasting, hydrolysis assisted solidifications, etc can be mentioned. In all cases, the objective is to obtain a very homogenous green body in order to facilitate the preparation of defect free materials.

However, in other cases, stable suspensions of ceramic powders are prepared in order to produce dry powders especially conditioned for forming by pressing. In this case, the most critical issue is to avoid the formation of hard agglomerates that could lead to formation of defects in the final material which could not be removed during firing. Two drying techniques are especially suitable for this purpose; spray drying and freeze-drying.

Spray-Drying vs. freeze drying

The two main drying techniques for obtaining ready to press powders are spray drying and freeze drying. In spray drying process, the solvent is eliminated by evaporation when the slurry is passed through a chamber at a temperature over the solvent boiling point, whereas during freeze drying the suspension is previously frozen and then water is removed by sublimation. The two processes are similar, except for energy flow. In the case of spray drying, energy is applied to the droplet, forcing evaporation of the medium resulting in both energy and mass transfer through the droplet. In spray freeze drying, energy only is removed from the droplet, forcing the melted to solidify. Both techniques are schematized in figure 3.2.

Spray drying is the most widely used industrial process involving particle formation and drying. It is highly suited for the continuous production of dry solids in either powder, granulate or agglomerate form from liquid feedstocks as solutions, emulsions and pumpable suspensions.

There are three fundamental steps involved in spray drying.

1. Atomization of a liquid feed into fine droplets.
2. Mixing of these spray droplets with a heated gas stream, allowing the liquid to evaporate and leave dried solids.
3. Dried powder is separated from the gas stream and collected.

Spray drying involves the atomization of a liquid feedstock into a spray of droplets and contacting the droplets with hot air in a drying chamber.
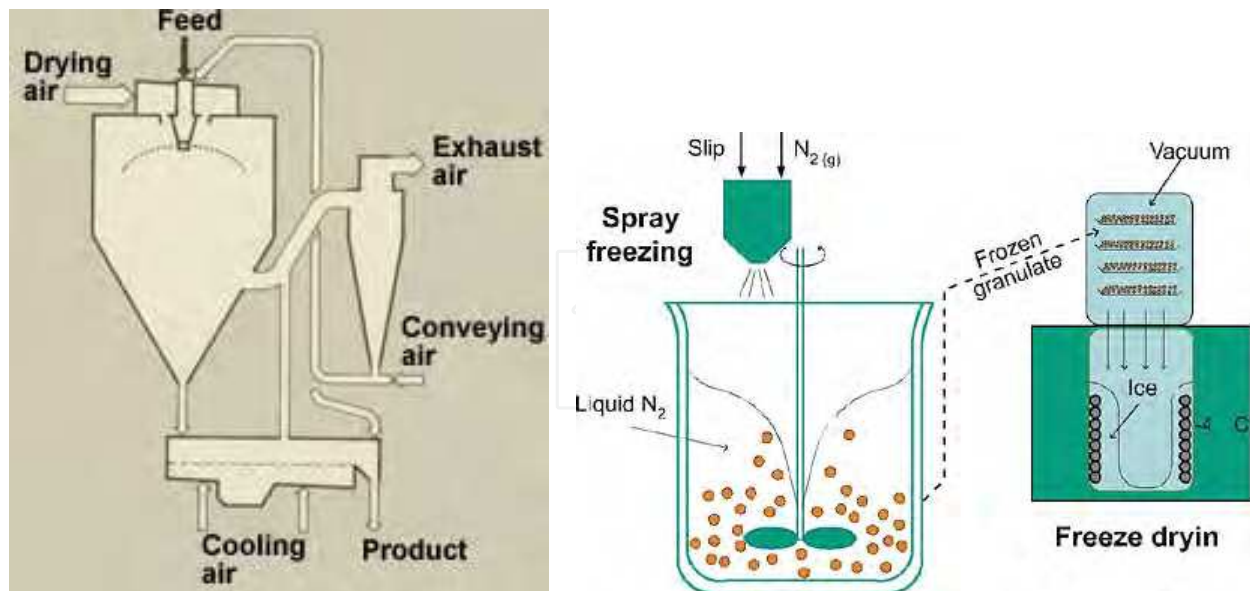
Fig. 3.2. Spray-drying and freeze–drying processes.

The sprays are produced by either rotary (wheel) or nozzle atomizers. Evaporation of moisture from the droplets and formation of dry particles proceed under controlled temperature and airflow conditions. Powder is discharged continuously from the drying chamber. Operating conditions and dryer design are selected according to the drying characteristics of the product and powder specification.

Spray formation is usually coupled to freeze drying process. This technique is named spray freeze drying. This process consists of

1. Atomization of liquid solutions or suspension using ultrasound, one-or two fluid nozzles or vibrating orifice droplet generators
2. Freezing of the droplets in a cryogenic liquid or cryogenic vapour
3. Ice sublimation at low temperature and pressure or alternatively atmospheric freeze-drying using a cold desiccant gas stream

The advantage of using conditioned powder for obtaining transparent ceramic materials is known (I. Amato et al., 1976). The enhanced behaviour during compaction of spray dried or freeze dried powders leads to a more homogeneous distribution of particles in the green body and finally a reduction in the residual porosity of the material. Nevertheless, the incorporation of additives during slurry preparation or binders for favouring soft granulation of powders makes an additional process before firing necessary. This process is named debinding.

Binders, which are used in the slip casting process or in pressing, give the green body a sufficient strength by gluing together particles at their boundary surfaces. Usually those binders are based on polyvinyl alcohols (PVA), polyacrylate or cellulose. High-polymeric compounds such as cellulose and polysaccharides work as plastification agents. They make the flow of ceramic masses during extruding possible.

The thermal treatment of the debinding process destroys the polymers by oxidation or combustion in oxygen containing atmosphere. Very often it is an uncontrolled reaction of

high reaction rate inside the shaped part creating a high gas pressure, which can lead to ruptures of the compact. Debinding process is schematized in figure 3.3.
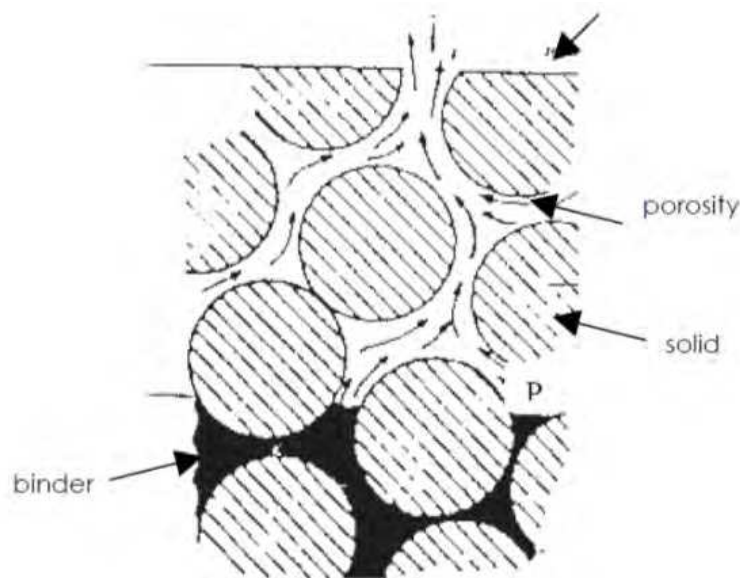

Fig. 3.3. Description of debinding process.

Debinding process is a critical step. In order to overcome the problems in thermal debinding, solvent debinding has been widely adopted by industry. In this process, a portion of the binder can be chemically removed by using solvents like acetone, trichloroethane or heptane. A large amount of open porosities, after solvent debinding, allows the degraded products to diffuse to the surface easily. A more environmentally friendly method is given by binder compositions containing water-soluble components, like polyethylene glycol.

Sintering

Finally, the green body is sintered by heating at high temperature in order to eliminate porosity and obtain the desired microstructure. The driving force for sintering is the reduction in surface free energy of the consolidated mass of particles. This reduction in energy can be accomplished by atom diffusion processes that lead to either densification of the body (by transport matter from inside the grains into the pores) or coarsening of the microstructure (by rearrangement of matter between different parts of the pore surfaces without actually leading to a decrease in the pore volume). The diffusion paths for densification and coarsening are shown in figure 3.4 for an idealized situation of two spherical particles in contact. The densification processes remove material from the grain boundary region leading to shrinkage whereas coarsening processes produce microstructural changes without causing shrinkage.
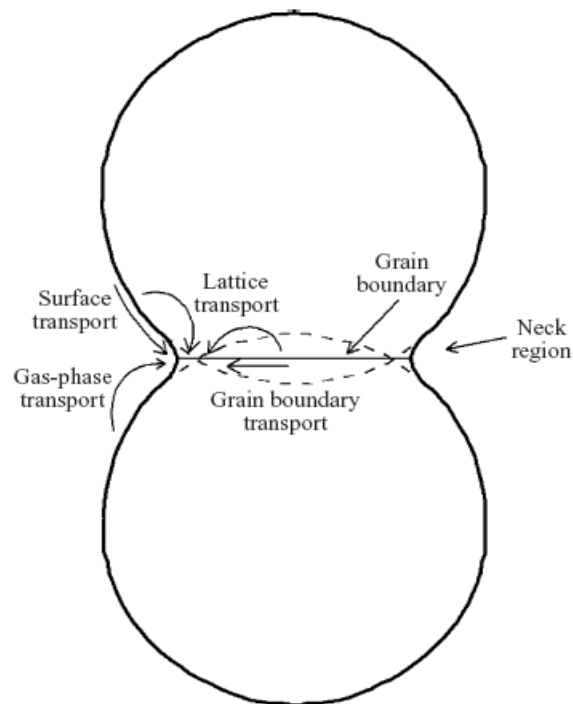
Fig. 3.4. Schematic representation of phenomena involved during firing of ceramics.

When the objective is to obtain transparent materials, it is necessary to control the microstructure evolution during ceramic sintering. The grain growth that occurs during sintering reduces the optical transmittance due to two reasons. Firstly, the pore size distribution in the sintered material is proportional to average grain size. Secondly, in the case of birefringent materials as alumina, the higher the grain size the more important the light scattering.

Grain growth inhibition can be attained by different methods. The most common strategies for reducing grain growth during sintering are the design of complex sintering cycles as two step sintering or the use of dopants for blocking coarsening mechanisms. Two-step sintering has been reported for preparing nanograin ceramics. In the process, the sample is first heated to a higher temperature to achieve an intermediate relative density (above 75%), and then rapidly cooled down and held at a lower temperature until it is fully dense (Z. Chen et al., 2008).

On the other hand, additives can impede the grain growth of ceramics during sintering. In particular, there are many studies treating the alumina grain growth inhibition using different dopants (S.J. Bennison et al., 1990a) (I. Alvarez et.al, 2010). An innovative method

for controlling alumina grain growth is described by M. Suárez et al., (2011). In this case, the dopant used is an alumina precursor in order to obtain pure alumina after sintering. The effect of alumina precursor doping on process kinetics and microstructure evolution is discussed.

However, the residual porosity of materials after conventional sintering is usually high enough to reduce noticeably their transmittance or even lead to opaque materials. Thus, an additional process for removing that porosity is usually needed. An effective method for attaining complete densification is the post-HIP treatment. In hot isostatic pressing, the sample predensified, until only closed porosity is present, is placed in a pressure vessel. The pressurizing gas is introduced by means of a compressor to achieve a given initial gas pressure, and the sample is heated to the sintering temperature. During this time the gas pressure increases further to the required value and collapses around the sample, thereby acting to transmit the isostatic pressure to the sample. The use of this technique for improving transparency has been shown by different authors (K. Itatani et al., 2006 and M. Suárez et al., 2010).

Pressure assisted sintering techniques

The simultaneous application of pressure and heat is also used in the Hot-Pressing and Spark Plasma Sintering, methods that are known as pressure assisted sintering techniques. In this case, a mechanical uniaxial pressure is applied to the sample placed in a dye by a vertical piston while the system is heated. Graphite is the most common die material because it is relatively inexpensive, is easily machined, and has excellent creep resistance at high temperatures. The rate of densification can be deduced by following the piston displacement. Typically, in Hot- Pressing, the sintering temperature is chosen to achieve full densification in 30 min to 2 h. Some guidance for selecting the appropriate hot pressing temperature may be obtained from pressure sintering maps, but trial and error is usually done. Pressure is often maintained during the cooldown step.

A sintering method with a configuration similar to Hot-Pressing has been recently developed. It is named Spark Plasma Sintering (SPS) and its main characteristic is that a pulsed DC current is directly passed through the graphite die while uniaxial pressure is applied. The characteristics include (a) high heating rate, (b) the application of a pressure, and (c) the effect of the current. The main advantage in comparison with other sintering techniques is the high heating rates that can be applied during sample sintering. The description of SPS process and a comparison of cycle duration with Hot Pressing are shown in figures 3.5 and 3.6

These features have a great influence on the characteristics of the materials obtained. The extremely short processing times allow obtaining special microstructures in the final material that are unattainable by other sintering techniques. Thus, it is possible to fabricate a dense material with an average grain size similar to starting powders. There are many scientific works showing the potential of this technique for obtaining a wide diversity of transparent polycrystalline materials (B. N. Kim et al., 2007), (C. Wang et al., 2009), (G. Zhang et al., 2009), (R. Chaim et al., 2006). Nowadays, one of the challenges related with this technique is the scaling-up in order to obtain large samples or complex shape components.
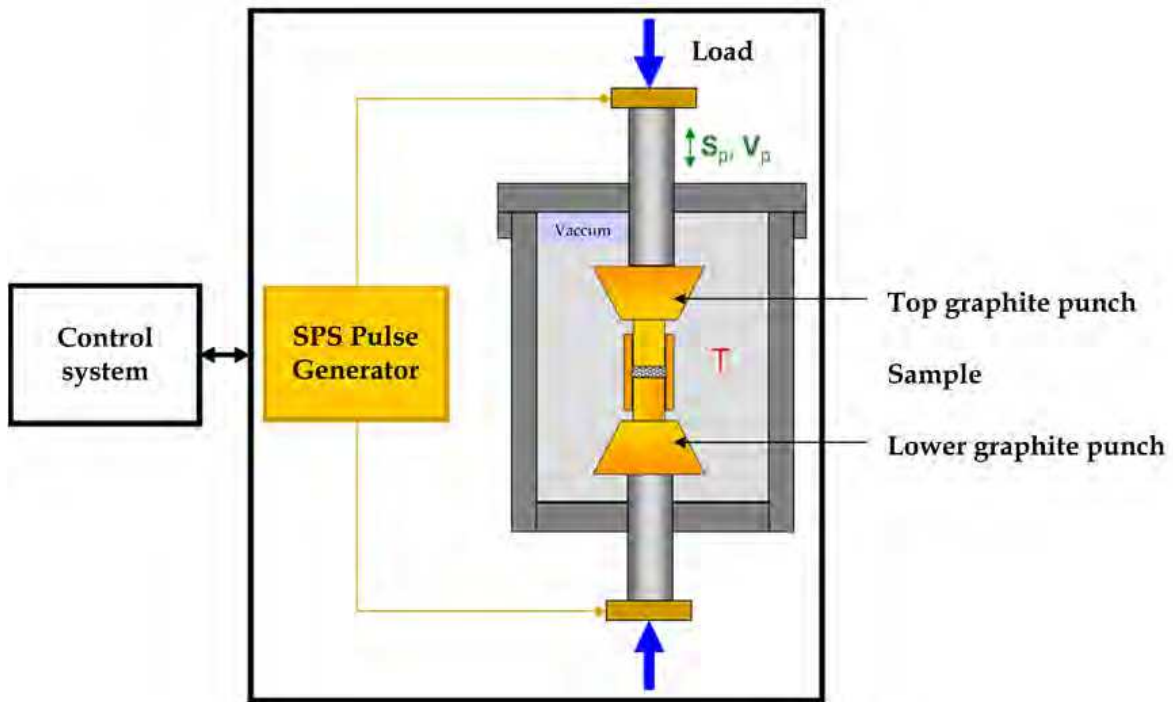
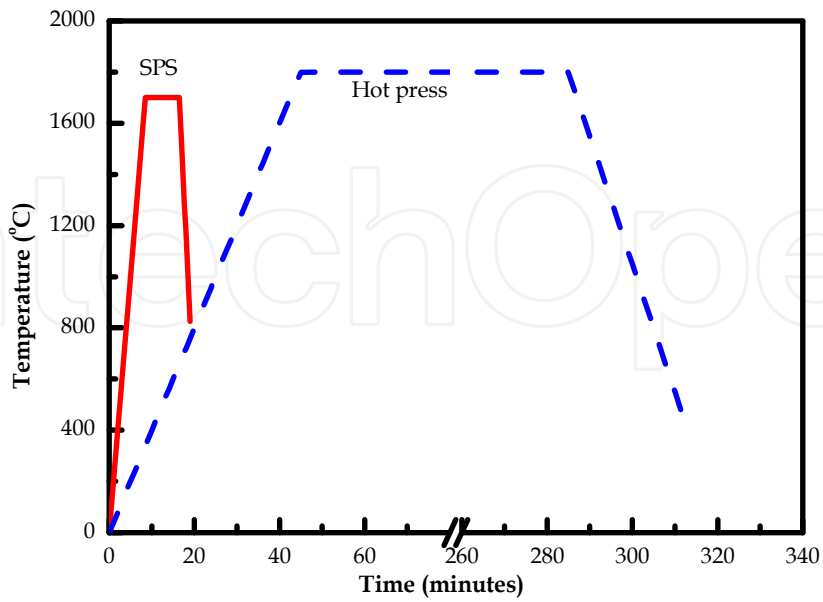Fig. 3.5. Description of SPS process.

Fig. 3.6. Comparison of cycle duration between Hot-Pressing and Spark Plasma Sintering

4. Characterization of transparent materials

Transparency represents the ability of materials to allow the transmission of light through them. When traversing a transparent material, a light beam propagates along the same direction before and after traversing the material (see Fig. 4.1a). However, perfectly transparent materials are rare in nature and most of them present the so-called scattering centres. When the concentration of scattering centres is sufficiently large, the material still allows the transmission of light, but the transmitted light beam does not only propagate along the incident direction, but diffuse, off-scattered, beams can be detected; in this case the material becomes translucent (see Fig. 4.1b). In this work, we shall refer only to the transparency of a material, which is measured as the real in-line transmittance. When the amount of scattering centres is higher, the materials scatter so much light that they become opaque (see Fig. 4.1c).
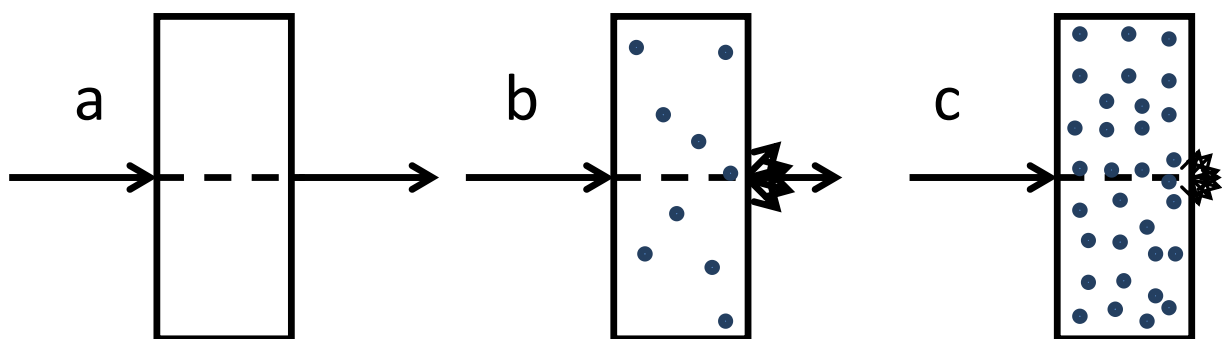

Fig. 4.1. Light propagation through a transparent (a), a translucent (b) and a highly dispersive, almost opaque (c) material.

Therefore, it becomes necessary to define a measurement technique that allows distinguishing between translucency and transparency. In this case, the relevant parameter is the real in line transmittance (Appetz & Bruggen, 2003) or RIT. In this case, a collimated light beam impinges on the sample and the detector is placed far away, usually 1 m, from the sample. This way, for ordinary detectors and light beams, the light scattered > 0.5° will not be detected. Any non-absorbing material must be spatially homogeneous with respect to its dielectric properties in order to become transparent. From an electromagnetic point of view, a defect, or scattering centre, is a spatial region in which a difference in the diagonal dielectric constant (refractive index) is present. The effect of dielectric heterogeneities is manifested through light scattering phenomena, which leads to losses both in the optical quality of the materials and in the total transmitted energy. In ceramics, the main scattering sources are given by the presence of pores, second phase inclusions, rough interfaces… (see Fig. 4.2). Whereas the roughness at interfaces can be minimized by an adequate polishing of the surfaces and the presence of second phases can be also made negligible by selecting pure materials, the presence of pores and the effects of grain boundaries can only be minimized by an adequate processing and sintering. In most cases, and particularly in cubic materials such as yttria, YAG, AlON, spinel, pores are by far the main source of scattering and most of the efforts in the literature have been devoted to minimization of this kind of scattering. In

non-cubic materials, of which alumina is the most intensively studied material, there is an additional scattering given by the dependence of the value of the refractive index with the orientation of the crystalline grain, which we shall refer to hereafter as scattering due to grains.
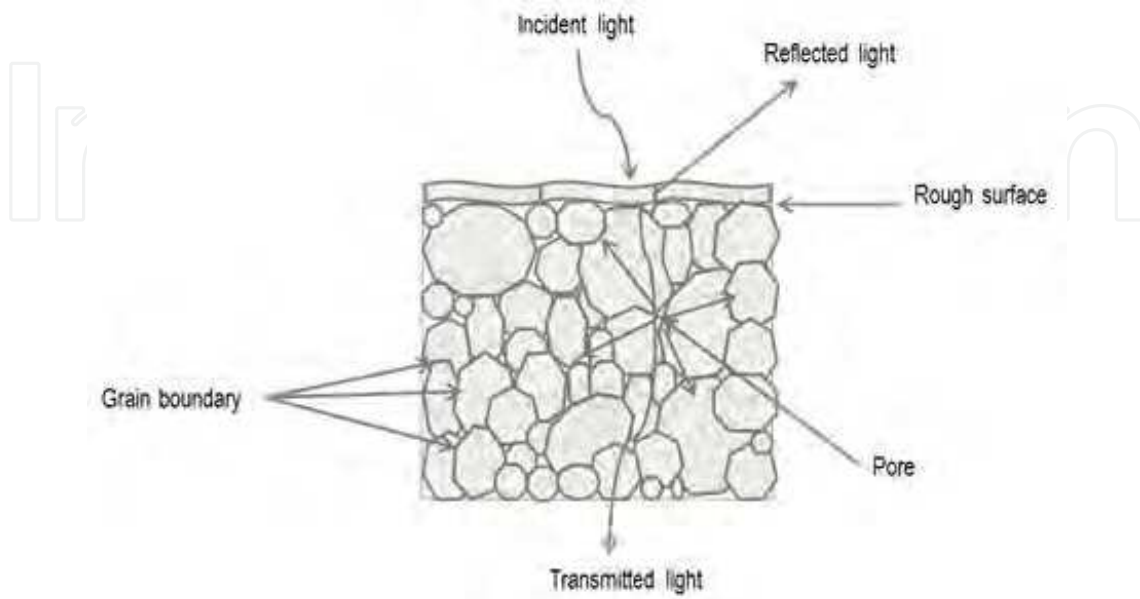

Fig. 4.2. Light scattering sources in polycrystalline ceramics.

Whenever a light beam reaches a surface separating two media with different refractive indices (see Figure 4.3), it deviates according to the Snell's law:

$$n_1 \cdot \sin\theta_1 = n_2 \cdot \sin\theta_2 \tag{1}$$
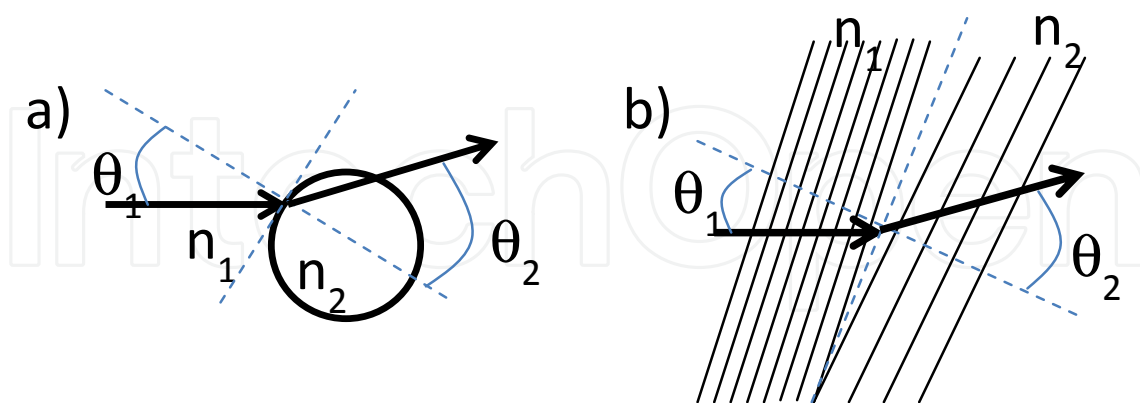
Fig. 4.3. Light refraction at (a) a matrix-pore boundary and (b) between two grains with different crystallographic orientations in a birefringent polycrystalline material.

A model based on geometrical optics was first produced by A. L. Dalisa and R. J. Seymour in which a spread function describing the effect on an incident collimated beam of randomly oriented spatial regions with a difference in the refractive index between zero and $\pm \Delta n_{max}$

was developed for ferroelectric ceramics (Dalisa & Seymour, 1973). This model was further applied by R. Appetz et al. to study the off-specular transmittance in polycrystalline alumina (Appetz & Bruggen, 2003), a birefringent material for which n_1 can be taken as 1.768 and n_2 as 1.76. Considering a grain boundary placed at 45°, the deviation of the light beam at this interface is calculated to be around 0.26°. If a beam light traverses a 1 mm thick polycrystalline alumina sample, in which the grain size is around 0.5 μm, the number of refractions that a light beam undergoes is not below several thousands. This gives an idea of the large scattering undergone by the beam. This discussion also illustrates why the larger the number of pores (for the same pore size), the smaller the real in line transmittance. However, following the same reasoning, one would expect the real in line transmittance to be higher for increasing grain size, whereas the experimental observations (Appetz & Bruggen, 2003) indicate that the amount of light scattered out of the normal incidence is larger in a sample with a grain size of 20 μm than in one with a grain size of 1 μm (Figure 4.4). This indicates that the geometrical model used above is not valid anymore to study the scattering of objects with dimensions of the order of the wavelength of the light.
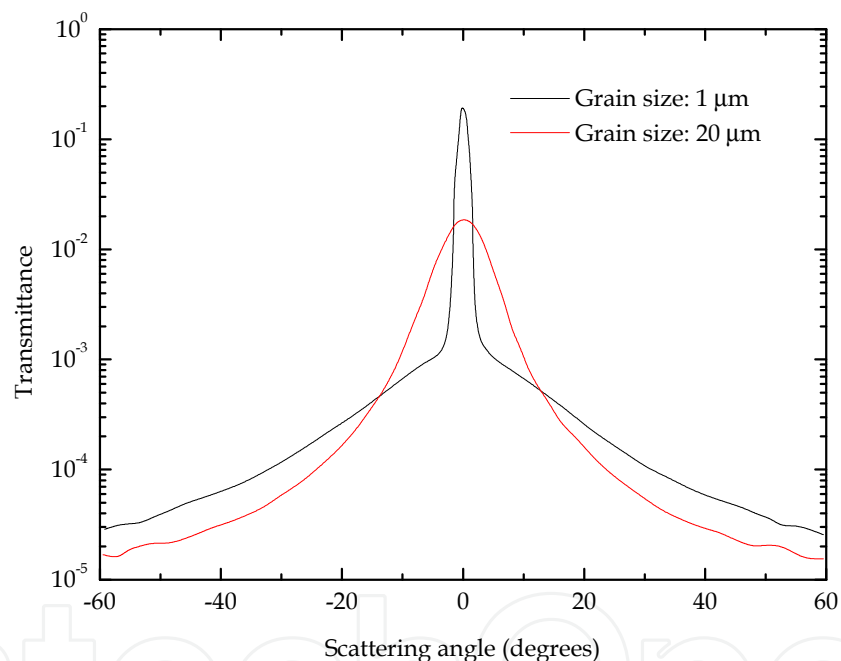

Fig. 4.4. Angular scattering profiles corresponding to 0.8 mm thick polycrystalline alumina samples with 1 μm (solid line) and 20 μm (dotted line) grain size (taken from Appetz & Bruggen, 2003).

In systems with a few defects and by using the Mie equation (Mie, 1908), it is possible to determine the intensity and directionality of the scattered radiation. This formulation is derived from the Maxwell equations and it is, therefore, valid for arbitrary defect sizes. However, as the Mie equation is complex to handle, it becomes helpful to use approximations. Two approximations are often used (Bohren & Huffmann, 2010; van de Hulst, 1957): Rayleigh-Gans-Debye scattering for large particles: $2\pi r \gg \lambda$ and Rayleigh scattering for small particles: $2\pi r \ll \lambda$, with r being the radius of the scattering centre. When dealing with transparent materials or materials close to transparency, the number of pores

and their dimensions verifies the conditions for the second approach (Rayleigh scattering) and, therefore, we'll focus our analysis under that simplification. According to this well-known approach, the intensity of electromagnetic radiation with wavelength λ scattered by an object of diameter d and refractive index n, at a distance R and angle of scattering θ is given by:

$$I = I_0 \frac{1+cos^2\theta}{2R^2}\left(\frac{2\pi}{\lambda}\right)^4\left(\frac{n^2-1}{n^2+2}\right)^2\left(\frac{d}{2}\right)^6 \tag{2}$$

The Rayleigh scattering cross section for a single particle can be expressed as:

$$\sigma_s = \frac{2\pi^5}{3}\frac{d^6}{\lambda^4}\left(\frac{n^2-1}{n^2+2}\right)^2 \tag{3}$$

In case a group of N scattering particles is considered, the scattering cross section is given by N times the single scattering cross section. This implies that the scattering due to pores of diameter d in a ceramic is much larger, by a factor of 2^6, than that due to pores of diameter d/2. If the size of the pores is reduced to half the initial size, the individual scattering is reduced by a factor of 2^6, whereas the number of scattering centres must be increased by a factor 2^3 if the total porosity is kept constant. This implies that, in total, by reducing the pore size by a factor of 2, the total dispersion is reduced by a factor 2^3, almost an order of magnitude. Therefore, in order to improve the real in line transmittance, two approaches can be followed: the porosity is strongly reduced or, as shown above, the size of the pores is kept much smaller than the wavelength of the radiation used.

Since the pioneering works by Peelen and Metselaar (Peelen and Metselaar, 1974), lots of efforts have been devoted to analyse and model the effects of the different scattering sources on the real in line transmittance. It is well known that the real in line transmittance decays exponentially with thickness, d, according to:

$$RIT = (1 - R_s)^2 \cdot \exp(-\gamma d) \tag{4}$$

where γ, the total scattering, is the sum of the scattering coefficients due to grains and pores: $\gamma = \gamma_{gb} + \gamma_p$. On the other hand, R_s accounts for the total reflected light at the air-material and material-air boundaries. It is well known that the amount of light reflected from a surface between two media (Born & Wolf, 2005) with refractive indices n_1 and n_2 at normal incidence is given by $R_s=(n_1-n_2)^2/(n_1+n_2)^2$. In this case, one of the media is air ($n_1=1$) and the other medium is the material under study ($n_2=n$). R. Appetz and M. P. B. van Bruggen calculated the light scattering coefficients due to pores and different grain orientations in non-cubic materials, considering just one pore size and one grain size (Appetz & Bruggen, 2003). The expressions given for those coefficients are:

$$\gamma_{gb} = \frac{3r_{gb}\pi^2}{\lambda_0^2}\Delta n_{gb}^2 \text{ and } \gamma_p = \frac{p}{\frac{4}{3}\pi r_p^3}\frac{3r_p\pi^2}{\lambda_0^2}\Delta n_p^2 \tag{5}$$

where r_{gb} (r_p) is the radius of the grain (pore); Δn_{gb}^2 (Δn_p^2) is the difference in the refractive indices between grains in birefringent materials (pore and matrix); p is the total porosity of the material and λ_0 is the wavelength of light used in vacuum. More recently, this analysis was extended to a distribution of pore and particle sizes (Suarez et al., 2009). In Figure 4.5,

the effect of considering a distribution of pores instead of a single pore is given. For this simulation, a Poisson pore size distribution with an average radius of 30 nm was taken into account. It can be observed that the main differences take place at short wavelengths, that is, in the visible part of the spectrum for the numbers considered in this example.
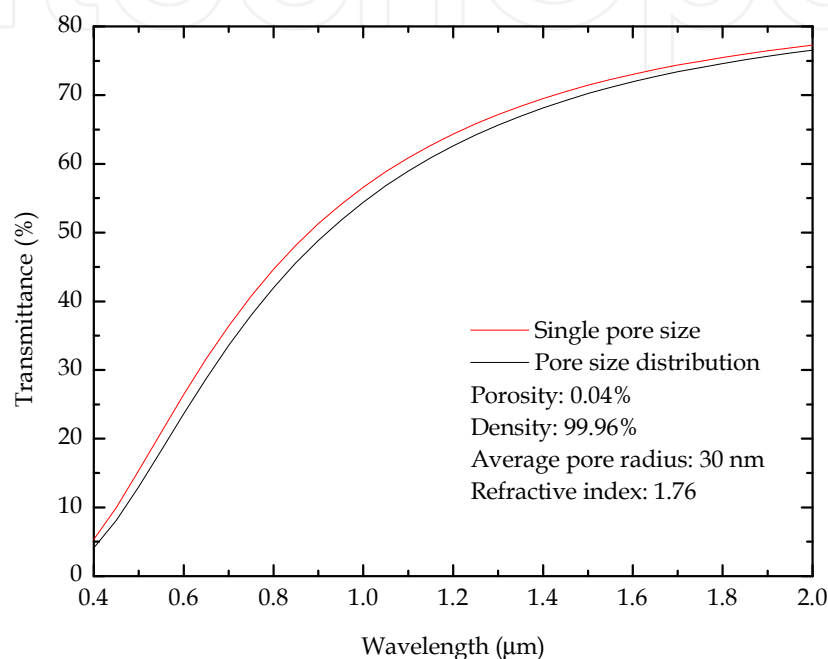

Fig. 4.5. Transmittance spectra in a material with a single pore size or a Poisson distribution of pore sizes.

In Figure 4.6, the effect of changing both the porosity for a fixed pore size (4.6.a) and the pore size at a fixed porosity (4.6.b) is simulated according to the formalism developed by Suarez et al. (Suarez et al., 2009). Some remarkable features should be highlighted: as shown in Figure 4.6.a, for a pore radius of 10 nm, in a 1 mm thick material and at a wavelength of 600 nm, i. e., in the visible range, a porosity of 0.5%, which corresponds to a density of the material of 99.5%, implies that the RIT decays to almost zero. Actually, values of the porosity over 0.3% lead to RIT values so small that their detection becomes very complicated for usual detectors. On the other hand, at the same wavelength and considering a porosity of only 0.05%, which corresponds to a density of 99.95%, it is shown that pore sizes over, approximately, 50 nm lead to very small RIT values. These two results combined imply that achieving a high density (>99.9%) is not usually enough to obtain a transparent material. It is also necessary to keep the values of pores below a given value that, according to these simulations, can be established below 30 nm.
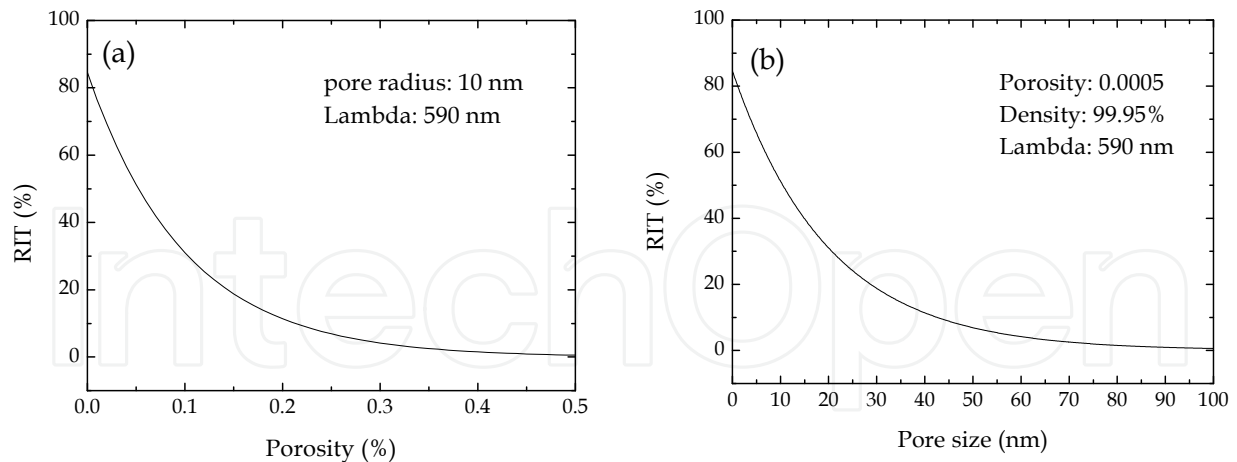
Fig. 4.6. Simulations considering different porosities and pore sizes.

The simulations shown above indicate the critical role of pores when transparent ceramics are being pursued. However, the situation can become more complex when the crystalline structure of the material considered is not cubic. In this case, the diagonal elements of the dielectric tensor will be, in general, different. In other words, the refractive index will depend on the crystalline orientation of each individual grain. For example, due to symmetry reasons, in alumina, two of the diagonal elements of the dielectric tensor are equal, but the third one is different ($\varepsilon_{xx}=\varepsilon_{yy}\neq\varepsilon_{zz}$). In alumina, this leads to a difference in the refractive index of only 0.008, but enough to induce a large scattering, particularly in the visible range. As shown in Figure 4.7a, the larger the grain size, the larger the scattering and, therefore, the smaller the RIT. Also, analogously to the porosity, the scattering becomes more critical at shorter wavelengths. It is shown in Figure 4.7a that whereas the RIT at 400 nm for a polycrystalline material does not reach 10%, it is close to 40% at 700 nm. Therefore, the grain size will be very important when materials are developed for the visible range and will not be so critical in devices operating in the infrared range. Following the same formalism, it can be shown that the RIT only falls to 60% at 1.5 microns and 70% at 2 microns when the average grain size is 2 microns in polycrystalline alumina. All RIT values shown so far have been calculated considering texture less materials. However, different routes have shown the possibility to induce some texture in the polycrystalline materials (Salem et al., 1989; Mao et al., 2008; Uchikoshi et al., 2004). Figure 4.7b shows how at two wavelengths, 400 and 700 nm, the RIT increases with increasing texture. In this simulation, texture = 0 corresponds to a perfectly polycrystalline material whereas texture = 1 corresponds to a fully textured, analogous to a single crystal, material. It is worth noting that no porosity has been considered in the simulations and that even so, at 400 nm, the RIT strongly decays from its maximum, around 80%, to only 20% due to a random orientation of the crystallites forming the material. The behaviour at 700 nm is similar, but the decay is not so abrupt, indicating again the strong wavelength dependence of the phenomenon. For these simulations, a grain size of only 500 nm has been considered, which is not easy to obtain in conventionally sintered alumina materials. Usual grain sizes are of the order of several μm, which leads to even more drastic reductions in the RIT, as can be deduced from Figure 4.7a.
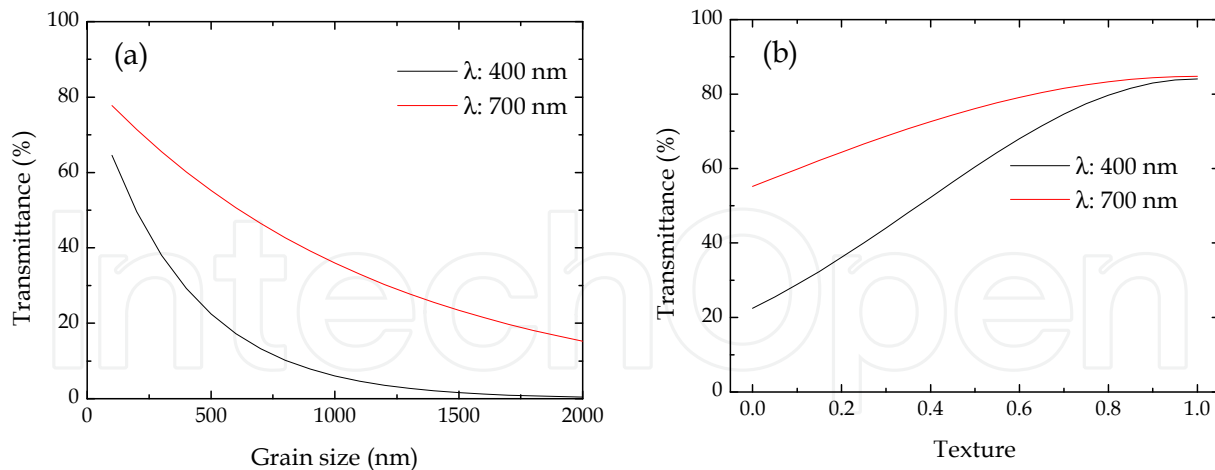
Fig. 4.7. Simulations for birefringent materials with different textures and grain sizes.

C. Pecharroman et al. developed a theoretical model (Pecharroman et al., 2009) for light scattering due to polycrystalline aggregates of uniaxial spheres within the Rayleigh-Gans-Debye approximation. This model shows that the scattering efficiency of each individual grain depends linearly on the grain size and on the texture of the samples. As indicated above, the most critical scattering is that due to the pores and this explains why common technical alumina ceramics which are considered dense at relative density over 99.5 % are opaque (white) when sintered in air, even if high purity raw materials are used. However, provided that the scattering due to pores decreases as $(d/\lambda)^4$, in order to make a material transparent it is not necessary to completely remove all the scattering centres, which is a cumbersome task, but it is enough to keep them all below a certain critical size. As an approximate rule, it is considered that the defects should be smaller than $\lambda/10$. In particular, for the visible range, in which the considered wavelengths range from 400 to 750 nm, the pore size should not be over a few tens of nm. Even so, the total porosity should never be over 0.05%. For this reason care must be taken not only during sintering, but also during processing and preparation of the green bodies. A uniform packing of the powders in green bodies has been shown in the literature to be critical to obtain low porosity ceramics. This is of particular importance when working with nanoceramics, as the attractive Van der Waals forces between particles are responsible for the high tendency of the nanoparticles to agglomerate. The presence of agglomerates leads to local differences in density which changes the sintering behaviour of the body leading to microcracks and microstructural effects such as residual pores and local coarsening and, therefore, to a large scattering. On the one hand, the raw powder should be very fine-grained in order to increase the sintering activity resulting in the elimination of residual porosity. Also, the structural homogeneity of sintering bodies is most important for a minimum of flaws that are detrimental to both optical and mechanical properties. This request for homogeneity makes the use of nanopowders < 100 nm still difficult. Casting methods are particularly suited to process raw powders with particle sizes between 100 and 150 nm.

Finally, it is obvious that preparing materials with the same thickness for a set of measurements is extremely difficult. For this reason, it is important to normalize

measurements to a given thickness. The expression that relates the transmittance at a normalized thickness d_1 considering a measurement performed on a material with a thickness d_2 is given by

$$\frac{T(d_1)}{(1-R_s)^2} = e^{-\gamma d_1} = e^{-\gamma d_1 \cdot \frac{d_2}{d_2}} = \left[e^{-\gamma d_2} \right]^{d_1/d_2} = \left[\frac{T(d_2)}{(1-R_s)^2} \right]^{d_1/d_2} \qquad (6)$$

5. Conclusions

In conclusion, the interest on transparent ceramic materials relies on the extraordinary combination of high mechanical performance, chemical resistance/inertness… and little or none absorption in different ranges of the electromagnetic spectrum from infrared to near ultra violet. It has been shown that obtaining a transparent ceramic material implies sintering to a density, very close to the theoretical density (≥99.9%), and keeping the few pores left with a pore size below 30 nm. In order to achieve this aim, attention must be paid not only to the raw materials: adequate granulometry, particle size… but it becomes also critical to control the packing of the powders in the green body. Usually, large defects present in the green bodies cannot be removed during the sintering process, and therefore, forming step is decisive for the preparation of transparent materials. Moreover, it has been shown how an adequate choice of the sintering technique combined with a tailoring of the starting powder is critical when an accurate control of the microstructural features is required. Finally, different analysis techniques of the transmittance spectra have been given from which average structural parameters such as pore size, porosity and grain size and texture in birefringent ceramics can be extracted.

6. References

Álvarez-Clemares I., Mata-Osoro G., Fernández A., López-Esteban S., Pecharromán C., Palomares J., Torrecillas R. & Moya J.S. (2010). Transparent alumina/ceria nanocomposites by spark plasma sintering. Advanced Engineering Materials, 12, 11, 1154-1160

Amato I., Baudrocco F. & Martorana D. (1976). Evaluation of freeze drying and spray drying processes for preparing transparent alumina. Material Science and Engineering, 26, 1, 73-78.

Anderson R.C. (1998). Transparent Yttria-based ceramics and method for producing same. U. S. Patent 3545987.

Appetz R. & Van Bruggen M.P.B. (2003). Transparent alumina: a light scattering model. Journal of the American Ceramic Society, 86, 3, 480-486.

Bennison S.J. & Harmer M.P. (1990a). A history of the role of MgO in the sintering of alfa-alumina. Ceramic Transactions, American Ceramic Society, 7, 13-49.

Bennison S.J. & Harmer M.P. (1990b). Effect of magnesia on surface diffusion in sapphire and the role of magnesia in the sintering of alumina. Journal of the American Ceramic Society, 73, 4, 833-837

Bohren C. F. & Huffmann D.R. (2010). Absorption and scattering of light by small particles, Wiley-Interscience, ISBN 3527406646, New York

Born M. & Wolf E. (2005). Principles of Optics-Electromagnetic theory of propagation, interference and diffraction of light, Cambridge University Press, ISBM 0521642221, Cambridge, UK.

Budworth D.W. (1970). The selection of grain-growth control additives for the sintering of ceramics. Mineralogical Magazine, 37, 291, 833-838.

Chaim R., Marder-Jaeckel R. & Shen J.Z. (2006). Transparent YAG ceramics by surface softening of nanoparticles in spark plasma sintering. Material Science and Engineering, 429, 1-2, 74-78

Cheng J., Agrawal D., Zhang Y. & Roy R. (2002). Microwave sintering of transparent alumina. Materials Letters, 56, 4, 587– 592.

Chen Z., Li J., Xu J. & Hu Z. (2008). Fabrication of YAG transparent ceramics by two-step sintering. Ceramics International, 34, 7, 1709-1712

Coble R. L. (1962). U.S. Pat. No.3 026 210.

Cook R., Kochis M., Reimanis I., Kleebe H. J. (2005). A new powder production route for transparent spinel windows properties: powder synthesis and windows properties. Proceedings of the Defense and Security Symposium.

Dalisa, A. L. & Seymour R. J. (1973). Convolution Scattering Model for Ferroelectric Ceramics and Other Display Media, Proceedings of the IEEE, 61, 7, 981–991.

Greskovich C. & Chernoch J.P. (1973). Polycrystalline ceramic lasers. Journal of Applied Physics, 44, 4599-4607.

Handwerker C.A., Morris P. A. & Coble R. L. (1989). Effects of chemical inhomogeneities on grain growth and microstructure in Al_2O_3. Journal of The American Ceramic Society, 72, 1, 130-136.

Hartnett T. M., Bernstein S. D., Maguire E. A., & Tustison R. W. (1998). Optical properties of AlON (aluminum oxynitride). Infrared Physics & Technology, 39, 4, 203–211.

Ikesue A., Furusato I. (1995). Fabrication of polycrystalline transparent YAG ceramics by a solid-state reaction method. Journal of the American Ceramic Society, 78, 1 225-228.

Itatami K., Tsujimoto T. & Kishimoto A. (2006). Thermal and optical properties of transparent magnesium oxide ceramics fabricated by post hot-isostatic pressing. Journal of the European Ceramic Society, 26, 4-5, 639-645

Kim B. N., Hiraga K., Morita K. & Yoshida H. (2007). Spark Plasma Sintering of transparent alumina. Scripta Materialia, 57, 7, 607-610

Kong, J., Tang, D.Y., Zhao B., Lu J., Ueda K., Yagi H. & Yanagitani T. (2005). 9.2-W diode-pumped $Yb:Y_2O_3$ ceramic laser. Applied Physics Letters, 86, 16, 16116-16119.

Mccauley J. W., Patel P., Chen M., Gilde G., Strassburger E., Paliwal B., Ramesh K.T. & Dandekar D.P (2099). AlON: A brief history of its emergence and evolution, Journal of the European Ceramic Society, 29, 2, 223-236.

Li J. G., Ikegami T., Lee J. H. & Mori T. (2000a). Low-temperature fabrication of transparent yttrium aluminum garnet (YAG) ceramics without additives. Journal of the American Ceramic Society, 83, 4, 961-963.

Li J. G., Ikegami T., Lee J. H., Mori T. & Yajima Y. (2000b). Co-precipitation synthesis and sintering of yttrium aluminum garnet (YAG) powders: the effect of precipitant. Journal of The European Ceramic Society, 20, 14-15, 2395-2405.

Lu T. C., Chang X. H., Qi J. Q., Lu X. J., Wei Q. M., Zhu S., Sun K., Lian J. & Wanga L. M. (2006). Low-temperature high-pressure preparation of transparent nanocrystalline $MgAl_2O_4$ ceramics. Applied Physics Letters, 88, 21, 213120-213123.

Lukin E. S., Vlasov A. S., Zubakhina M.A. & Datsenko A.M. (1980). Effect of γ radiation on the optical properties of transparent yttrium-oxide ceramics. Glass and Ceramics, 37, 5, 255-258.

Mah T. I., Parthasarathy T. A. & Lee H. D. (2004). Polycristalline YAG; structural of functional?. Journal of Ceramic Processing Research, 5, 4, 369-379.

Mao X., Wang S., Shimai S. & Guo J. (2008). Transparent Polycrystalline Alumina Ceramics with Orientated Optical Axes, Journal of the American Ceramic Society. 94, 10, 3431-3433.

Mie G. (1908). Beiträge zur Optik trüber Medien, speziell kolloidaler Metallösungen, Annalen der Physik. 330, 377–445.

Morita K., Kim B.N., Hiraga K., Yoshida H. (2008). Fabrication of transparent $MgAl_2O_4$ spinel polycrystal by spark plasma sintering processing. Scripta Materialia, 58, 12, 1114–1117.

Mouzon, J., Glowacki E. & Odén M. (2008). Comparison between slip-casting and uniaxial pressing for the fabrication of translucent yttria ceramics. Journal of Material Science, 43, 8, 2849-2856

Patel P.J., Gary A. G., Dehmer P. G. & McCauley J.W. Transparent Armor, The AMPTIAC Newsletter. Advanced Materials and Processes Technology, 4, 3, 1-24.

Pecharroman C., Mata-Osoro G., Diaz L. A., Torrecillas R. & Moya J. S. (2009). On the transparency of nanostructured alumina: Rayleigh-Gans model for anisotropic spheres, Optics Express 17, 8, 6899-6912.

Peelen J. G. J. & Metselaar R. (1974). Light Scattering by Pores in Polycrystalline Materials: Transmission Properties of Alumina, Journal of Applied Physics, 45, 1, 216-220.

Peuchert U., Okano, Y., Menke Y., Reichel S. & Ikesue, A. (2009). Transparent cubic-ZrO_2 ceramics for application as optical lenses. Journal of the European Ceramic Society, 29, 2, 283-291.

Qin G., Lu J., Bisson J. F., Feng Y., Ueda K. I., Yagi H. & Yanagitani T. (2004). Upconverion luminescence of Er^{3+} in highly transparent YAG ceramics. Solid State Communications, 132, 2, 103-106.

Salem J. A., Shannon Jr J. L. & Brad R. C. (1989). Crack Growth Resistance of Textured Alumina, Journal of the American Ceramic Society. 72, 1, 20-27.

Savastru D., Miclos S., Cotïrlan C., Ristici E., Mustata M., Mogïldea M., Mogïldea G., Dragu T. & Morarescu R. (2004). Nd:YAG Laser system for ophthalmology: Biolaser-1. Journal of Optoelectronics and Advanced Materials, 6, 2, 497–502.

Shikao S. & Jiye W. (2001). Combustion synthesis of Eu activated $Y_3Al_5O_{12}$ phosphor nanoparticles. Journal of Alloys and Compounds, 327, 1-2, 82–86.

Shuzhi L., Bangwei Z., Xiaolin S., Yifang O., Haowen X. & Zhongyu X. (1999). The structure and infrared spectra of nanostructured $MgO-Al_2O_3$ solid solution powders prepared by the chemical method. Journal of Materials Processing Technology, 89-90, 405-409.

Suarez M., Fernandez A., Menendez J.L. & Torrecillas R. (2009). Grain growth control and transparency in spark plasma sintered self-doped alumina materials. Scripta Materialia 61, 10, 931-934.

Suárez M., Fernández A., Menéndez J.L., Nygren M., Torrecillas R. & Zhao Z. (2010). Hot Isostatic pressing of optically active Nd:YAG powders doped by a colloidal processing route. Journal of the European Ceramic Society, 30, 6, 1489-1494

Suárez M., Fernández A., Menéndez J.L. & Torrecillas R. (2011). Blocking of grain reorientation in self-doped alumina materials. Scripta Materialia, 64, 6, 517-520

Takaichi K., Yahi H., Lu J., Shirakawa A., Ueda K., Yanagitani T. & Kaminskii A.A. (2003). Yb^{3+} doped $Y_3Al_5O_{12}$ ceramics- A new solid-state laser material. Physics state solid A, 200, 1, R5-R7.

Tokurakawa, M.T., Kazunori S., Akira U., Ken-ichi Y., Hideki Y., Takagimi K. & Alesander A. (2007). Diode-pumped 188 fs mode-locked Yb^{3+}:Y_2O_3 ceramic laser, Applied Physics Letters, 90, 7, 071101-071104.

Uchikoshi T., Suzuki T.S., Okuyama H. & Sakka Y. (2004). Control of crystalline texture in polycrystalline alumina ceramics by electrophoretic deposition in a strong magnetic field, Journal of Materials Research, 19, 5, 1487-1491.

Van de Hulst H. C. (1957). Light scattering by small particles, John Wiley and Sons, ISBN 0486642283, New York.

Wang C. & Zhao Z. (2009). Transparent $MgAl_2O_4$ ceramic produced by spark plasma sintering. Scripta Materialia, 61, 2, 193-196

Wei C. G. (2009). Transparent ceramis for lighting. Journal of the European Ceramic Society, 29, 2, 237-244.

Wen L., Sun X., Xiu Z., Chen S. & Tsai C .T. (2004). Synthesis of nanocrystalline yttria powder and fabrication of transparent YAG ceramics. Journal of the European Ceramic Society, 24, 2681-2688.

Zhang G., Wang Y., Fu Z., Wang H., Wang W., Zhang J., Lee S.W. & Niihara K. (2009). Transparent mullite ceramic from single-phase gel by spark plasma sintering. Journal of the European Ceramic Society, 29, 13, 2705-2711
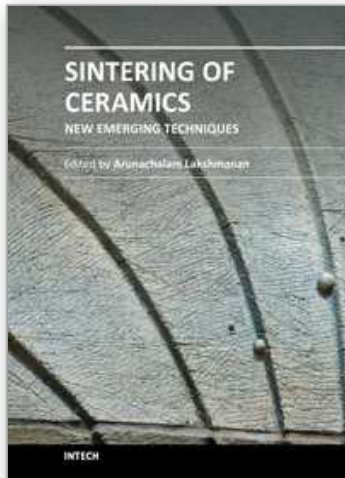
Sintering of Ceramics - New Emerging Techniques

Edited by Dr. Arunachalam Lakshmanan

The chapters covered in this book include emerging new techniques on sintering. Major experts in this field contributed to this book and presented their research. Topics covered in this publication include Spark plasma sintering, Magnetic Pulsed compaction, Low Temperature Co-fired Ceramic technology for the preparation of 3-dimesinal circuits, Microwave sintering of thermistor ceramics, Synthesis of Bio-compatible ceramics, Sintering of Rare Earth Doped Bismuth Titanate Ceramics prepared by Soft Combustion, nanostructured ceramics, alternative solid-state reaction routes yielding densified bulk ceramics and nanopowders, Sintering of intermetallic superconductors such as MgB2, impurity doping in luminescence phosphors synthesized using soft techniques, etc. Other advanced sintering techniques such as radiation thermal sintering for the manufacture of thin film solid oxide fuel cells are also described.

How to reference

In order to correctly reference this scholarly work, feel free to copy and paste the following:

INTECH

open science | open minds